

The glycotope-specific RAV12 monoclonal antibody induces oncosis *in vitro* and has antitumor activity against gastrointestinal adenocarcinoma tumor xenografts *in vivo*

Deryk Loo, Nancy Pryer, Peter Young, Tony Liang, Suzanne Coberly, Kathleen L. King, Key Kang, Penny Roberts, Mary Tsao, Xiaolin Xu, Beverly Potts, and Jennie P. Mather

Raven Biotechnologies, Inc., South San Francisco, California

Abstract

RAV12 is a chimeric antibody that recognizes an N-linked carbohydrate antigen (RAAG12) strongly expressed on multiple solid organ cancers. More than 90% of tumors of colorectal, gastric, and pancreatic origin express RAAG12, and a majority of these tumors exhibit uniform RAAG12 expression. RAV12 exhibits potent cytotoxic activity *in vitro* against COLO 205 colon tumor cells via an oncotic cell death mechanism. RAV12-treated COLO 205 cells undergo morphologic changes consistent with oncosis, including cytoskeletal rearrangement, rapid plasma membrane swelling, and cell lysis. RAV12 inhibited the growth of RAAG12-expressing gastrointestinal tumor xenografts in athymic mice. In the case of SNU-16 tumor cells, twice weekly treatment of established s.c. tumors with 10 mg/kg RAV12 caused a ~70% suppression of tumor growth at the end of the study. This preclinical data has led to the initiation of a phase I/IIA clinical study of RAV12 in patients with metastatic or recurrent adenocarcinoma. [Mol Cancer Ther 2007;6(3):856–65]

Introduction

The clinical success of monoclonal antibody therapeutics, such as rituximab, trastuzumab, cetuximab, and bevacizumab, validates the use of monoclonal antibodies as antitumor agents. Antibody therapeutics can confer antitumor effects via multiple mechanisms. Antibodies

can deliver chemotherapeutic agents; they can target and activate host cell effector functions; and in some instances, they can bind and elicit antiproliferative or cytotoxic activities directly upon target cells. Because of the genetic variability of tumors, antibodies with multiple effector mechanisms may be needed to achieve maximal antitumor effects. Although eight monoclonal antibodies are marketed for use in treating cancer, there continues to be a great need for potent tumor selective therapeutic antibodies with unique antitumor mechanisms.

We are using a cell-based immunization approach to generate therapeutic antibodies against surface expressed targets found on human fetal progenitor stem cell lines. The progenitor stem cell lines have the capacity to provide a rich source of novel oncofetal antigens (1–3). Many of these developmentally regulated oncofetal antigens may be re-expressed on rapidly growing cancer cells. The stem cell lines have been used as immunogens to generate panels of monoclonal antibodies directed against cell surface proteins expressed during specific stages of fetal development and overexpressed by human cancers. Using this approach, we identified a monoclonal antibody (KID3) as a candidate therapeutic agent. Initial studies showed KID3 bound to the cell surface of multiple solid organ adenocarcinomas, possessed cytotoxic activity *in vitro*, and exhibited antitumor activity in tumor xenograft models. Based on results from these studies, the chimeric monoclonal antibody RAV12 (IgG1 subclass) was generated for preclinical/clinical development.

Herein, we describe the biological properties of RAV12 and the parental murine KID3 monoclonal antibody. RAV12 recognizes a primate-restricted N-linked carbohydrate epitope, designated RAAG12, expressed on a number of human carcinomas. RAV12 exhibits cytotoxic activity *in vitro* against the RAAG12-expressing human colon tumor cell line COLO 205. Cells undergoing RAV12-induced cell death exhibit characteristics consistent with oncotic cell death (also called programmed cell necrosis; ref. 4), including sodium-dependent rapid cellular swelling and lysis. RAV12 exhibits potent antitumor activity against human colon, gastric, and pancreatic tumor xenografts in athymic mice. A phase I/IIA clinical study of RAV12 in patients with metastatic or recurrent adenocarcinoma has been initiated.

Materials and Methods

Cell Lines

The tumor cell lines COLO 201, COLO 205, SNU-16, A549, and SU.86.86 were obtained from the American Type

Received 9/18/06; revised 12/11/06; accepted 1/25/07.

The costs of publication of this article were defrayed in part by the payment of page charges. This article must therefore be hereby marked *advertisement* in accordance with 18 U.S.C. Section 1734 solely to indicate this fact.

Note: Current address for N. Pryer: Novartis Institute for Biomedical Research, 4560 Horton Street, Emeryville, CA 94608.

Requests for reprints: Deryk Loo, Raven Biotechnologies, Inc., 1140 Veterans Boulevard, South San Francisco, CA 94080. Phone: 650-624-2636; Fax: 650-553-9169. E-mail: dloo@ravenbio.com
Copyright © 2007 American Association for Cancer Research.
doi:10.1158/1535-7163.MCT-06-0581

Culture Collection (Manassas, VA). All cell lines were maintained in F12/DMEM (Invitrogen, Carlsbad, CA), supplemented with 10% fetal bovine serum (FBS; Hyclone, Logan, UT) in a humidified atmosphere of 95% air and 5% CO₂ at 37°C.

Animals

Female (for s.c. xenograft studies) or male (for subrenal capsule xenograft studies) athymic mice (CRL.nu/nu), 6 to 8 weeks of age, were purchased from Charles River Laboratories (Wilmington, MA). Mice were housed in specific pathogen-free conditions in accordance with U.S. Department of Agriculture guidelines. All studies were carried out under approved institutional experimental animal care and use protocols. Animals were provided pelleted food and water *ad libitum*.

Antibodies

The anti-Lewis^a (Le^a) antibody PR4D2 was obtained from Chemicon International (Temecula, CA). Antibodies to Le^b, Le^x, and Le^y were obtained from Calbiochem (San Diego, CA). Anti-Ca19-9 was obtained from Vector Laboratories (Burlingame, CA). Anti-Ca50 and anti-CA242 were obtained from Lab Vision (Ferment, CA). Mouse IgG was obtained from Jackson Immunochemicals (West Grove, PA).

Glyco-Analogues

The glyco-analogues and bovine serum albumin (BSA)-conjugated glyco-analogues were obtained from Dextra Labs (Reading, United Kingdom).

Generation of Murine KID3 Monoclonal Antibody and Chimeric RAV12 Antibody

The murine KID3 monoclonal antibody was generated by immunizing BALB/c mice in the foot pad with a mixture of intact, viable, human fetal kidney progenitor cells and Ribi adjuvant (Corixa, Hamilton, MT) over a period of 3 months. Antibody titer was monitored by flow cytometry using the human fetal kidney progenitor cells. Lymph nodes from mice showing sufficient titers were harvested, and isolated lymphocytes were fused with the mouse myeloma line X63-Ag8.653 (American Type Culture Collection) using standard methodologies (5).

To generate chimeric RAV12, cDNAs encoding the variable heavy and light domains of KID3 were cloned using standard recombinant DNA methodologies (6) and ligated into expression vectors containing human IgG1 and κ constant domains. RAV12 was expressed in a genetically engineered Chinese hamster ovary cell line (CRL-9096; American Type Culture Collection) using a proprietary serum-free culture medium. The protein was purified by multiple chromatography steps and available as a clear, sterile liquid.

Purification of RAAG12-Bearing Proteins from COLO 205 Cells

RAV12-reactive antigens were purified from COLO 205 cell lysate by passing the cell lysate over a KID3-conjugated Sepharose affinity resin column. KID3 was conjugated to *N*-hydroxysuccinimide-activated Sepharose 4 fast flow (Amersham Biosciences, Piscataway, NJ) according to the manufacturer's protocol. Econo-prep columns (Bio-Rad,

Hercules, CA) packed with 1 mL KID3-conjugated Sepharose were pre-eluted with 0.1 mol/L glycine HCl (pH 2.8; Sigma-Aldrich, St. Louis, MO) followed by 0.1 mol/L ethanolamine (pH 11.2; Sigma-Aldrich). Cell lysates were passed over the column; the column was washed extensively with lysis buffer and eluted with 0.1 mol/L ethanolamine (pH 11.2) followed by 0.1 mol/L glycine HCl (pH 2.8). Fractions were collected and neutralized with 1 mol/L Tris (pH 7.6; final concentration of 0.1 mol/L). Purified samples were precipitated with methanol/chloroform and resuspended in buffer for subsequent analysis.

Deglycosylation of RAAG12-Bearing Proteins

Purified protein samples were deglycosylated using the Enzymatic Deglycosylation kit and Deglycosylation Plus kit (ProZyme, San Raphael, CA) according to the manufacturer's protocol. Standard digestion period was 3 h at 37°C. Additional exoglycosidases or endoglycosidases were obtained from ProZyme. Deglycosylated samples were analyzed by SDS-PAGE and Western blotting.

Western Blot Analysis

RAAG12-bearing proteins purified from COLO 205 cell lysates were reduced with 2 mmol/L DTT (Pierce Biotechnology, Inc., Rockford, IL) and alkylated with 10 mmol/L iodoacetamide (Sigma-Aldrich), subjected to SDS-PAGE using Invitrogen/NOVEX 4% to 20% Tris-Glycine gels (Invitrogen, Carlsbad, CA), and transferred to nitrocellulose membranes (Invitrogen) according to manufacturer's protocol. Membranes were blocked with 5% nonfat dry milk in Tween-TBS [0.1% Tween 20 in 100 mmol/L Tris-Cl (pH 7.5), 0.9% NaCl] for 30 min, probed with KID3 at 2 μ g/mL in blocking buffer for 1 h, detected using an alkaline phosphatase-conjugated anti-mouse secondary antibody for 30 min (Jackson ImmunoResearch, West Grove, PA), and visualized using 5-bromo-4-chloro-3-indolyl phosphate/nitroblue tetrazolium substrate according to the manufacturer's protocol (Pierce Biotechnology). KID3 was used for the Western blot studies due to reagent availability. Subsequent studies with chimeric RAV12 showed equivalence to KID3.

Binding/Competition ELISA

The BSA-conjugated glyco-analogue lacto-*N*-fucopentose II (LNFPII; 2 μ g/mL) was immobilized onto NUNC Maxisorb 96-well plates (Rochester, NY) for 2 h at room temperature in HBSS. Plates were blocked for 30 min at room temperature with blocking buffer (5% BSA in HBSS). For direct antibody binding assays, 2 μ g/mL of antibody was incubated on the plate for 1 h at room temperature. For glyco-analogue competition assays, 2 μ g/mL KID3 or PR4D2 antibody was incubated with 100 μ g/mL glyco-analogues at 1:10 final volume for 30 min at 37°C, diluted to final volume, and incubated on the plate for 1 h at room temperature. Plates were washed with HBSS; secondary horseradish peroxidase-conjugated antibody was added and incubated for 30 min at room temperature (horseradish peroxidase-conjugated donkey anti-mouse IgG H+L from Jackson ImmunoResearch was used at 1:1,000 dilution). Plates were washed with HBSS and developed with 3, 3', 5, 5'-tetramethylbenzidine substrate according to

the manufacturer's protocol (KPL Laboratories, Inc., Gaithersburg, MD). KID3 was used for these ELISA studies due to technical constraints. Subsequent studies with chimeric RAV12 showed equivalence to KID3.

Tissue Immunohistochemistry

For the cancer and limited normal tissue surveys, sections were cut from frozen tumors (8 μm), formalin-fixed, paraffin-embedded (FFPE) tumors or normal tissues (4–5 μm), or obtained as pre-cut FFPE cancer tissue microarray slides. Frozen tumors were obtained from Ardais (Lexington, MA), Phenopath (Seattle, WA), Cureline (South San Francisco, CA), Oncotech (Tustin, CA), and D. Mangham (University of Birmingham, Birmingham, England). Normal tissues were obtained from Asterand (Detroit, WI). FFPE tumor specimens were obtained from Cureline, Asterand, and D. Mangham. FFPE cancer tissue microarray slides were obtained from Biogenex (San Ramon, CA.), Imgenex (San Diego, CA), Petagen (Seoul, South Korea), and Asterand. Tumor tissue sections were stained using the VectaStain Elite ABC kit (Vector Laboratories) with 5 $\mu\text{g}/\text{mL}$ biotinylated RAV12 according to the manufacturer's protocol with the following modifications. Antigen retrieval of FFPE sections was done by incubating slides in citric buffer (pH 6.0) in the DC2002 Decloaking Chamber Pro (Biocare Medical, Walnut Creek, CA) at 125°C for 30 s. Endogenous biotin was blocked by incubation for 30 min in 5% goat serum containing 0.1 mg/mL avidin followed by incubation in 30 $\mu\text{g}/\text{mL}$ d-biotin blocking solution for 30 min. Endogenous peroxidase was quenched by incubation with 3% hydrogen peroxide/methanol solution for 10 min. Frozen sections were fixed with a 50:50 mixture of acetone/ethanol before staining.

For the expanded normal tissue Good Laboratory Practice survey (Pathology Associates Division, Charles River Laboratory), biotinylated RAV12 (2–50 $\mu\text{g}/\text{mL}$) was applied to frozen human sections from autopsy or biopsy samples. Samples were stained as described above for the tumor tissue sections with the following modifications. Endogenous peroxidase was quenched by incubation of the slides with glucose oxidase (1 unit/mL) and sodium azide (1 mmol/L) for 1 h, and nonspecific protein binding was reduced by incubation with protein blocking solution [PBS (pH 7.2) containing 5% human γ -globulins, 5 mg/mL salmon sperm DNA, 0.5% casein, 1% BSA, and 1 mg/mL heat aggregated human IgG] for 1 h.

In vitro Alamar Blue Assay

COLO 205 cells were plated at 500 per well in 96-well plates in F12/DMEM containing 10% FBS. An equal volume of test antibody (diluted in F12/DMEM containing 10% FBS) was added to the wells, then the plates were incubated at 37°C for 4 days. Cell viability was determined using the Alamar Blue assay according to the manufacturer's protocol (Trek Diagnostics, Cleveland, OH).

Video Microscopy

COLO 205 cells were released from flasks with 10 mmol/L EDTA in PBS. A T25 flask (BD Falcon, Franklin Lakes, NJ) was seeded with 10,000 cells in F12/DMEM

containing 10% FBS. Antibodies were added at a final concentration of 20 $\mu\text{g}/\text{mL}$ immediately following plating, and the flask was placed on the stage of a Nikon Diaphot phase-contrast microscope housed within a 95% air/5% $\text{CO}_2/37^\circ\text{C}$ controlled chamber. Images were captured with an Optronics DEI470 CCD video camera (Goleta, CA) and recorded on tape with a Panasonic High Density Time Lapse Video Cassette Recorder AG6790 (Secaucus, NJ).

Cell Immunostaining

COLO 205 cells cultured in chamber slides in the presence of RAV12 antibody were washed with HBSS and fixed for 10 min at 4°C with 4% (w/v) paraformaldehyde/PBS (Sigma, St. Louis, MO). The fixed cells were washed with HBSS and blocked/permeabilized for 10 min at 4°C with HBSS containing 1% BSA and 0.5% Triton X-100. The permeabilized cells were then washed with blocking buffer (HBSS containing 1% BSA) and blocked for 1 h at 4°C. Blocked cells were stained with antibodies (2 $\mu\text{g}/\text{mL}$) for 1 h at room temperature, washed with blocking buffer, then incubated with Alexa Fluor-conjugated secondary antibodies (Invitrogen) for 30 min at room temperature in the dark. Stained cells were washed with blocking buffer followed by HBSS. Coverslips were mounted using Vectashield Hardmount mounting media with propidium iodide (Vector Laboratories). The slides were visualized using a Nikon Eclipse E-800 microscope.

Subrenal Capsule Xenograft Protocol

Human tumor-derived cells cultured *in vitro* were harvested with 10 mmol/L EDTA in PBS and resuspended in F12/DMEM containing 10% FBS. Cells (500,000 per implant) were resuspended in a 50- μL button of rat tail type I collagen and cultured *in vitro* overnight. The tumor cell-containing collagen buttons were placed under the kidney capsule of male athymic mice through a paralumbar surgical approach as previously described (7). Following 2 to 8 days of tumor cell establishment, monoclonal antibodies were administered i.p. thrice weekly for up to 2 weeks. Two days following the final dose, animals were sacrificed, and human tumors were recovered from the kidney capsules and photographed, then DNA was extracted and human DNA was quantified by the Taqman quantitative human DNA assay.

Taqman Quantitative Human DNA Assay

Human tumors were recovered from mouse kidney capsules, and total genomic DNA was isolated using the Promega Wizard SV Genomic DNA Purification kit according to the manufacturer's protocol (Promega, Madison, WI). The amount of human tumor DNA extracted from the subrenal capsule tumors was quantified by quantitative PCR using human-specific *RPL19* gene primers and probe (ref. 8; forward primer, 5'-CTTTCCTTTCGCTGCTGC; reverse primer, 5'-TAACCAGACCTTCTTCTT; probe, 5'-CCGACCCATGAGTATGCTC; Bioresearch Technologies, Inc., Novato, CA). Human DNA was amplified in a reaction containing 4 mmol/L MgCl_2 , 200 $\mu\text{mol}/\text{L}$ deoxy-nucleotide triphosphates, 250 nmol/L primers, 150 nmol/L probe, 5 units *Bst*XI, and 1.25 units Taq Gold in a Applied

Biosystems SDS 7000 machine according to the manufacturer's protocol (Applied Biosystems, Foster City, CA). The C_t values from experimental conditions were compared with the generated standard curve (human DNA input versus C_t value) to determine the quantity of human DNA present in each sample. The R^2 values for the standard curve were >0.95 ; all experimental C_t values were within the linear portion of the standard curve. Statistical analysis by ANOVA and Student's two-tailed t test were used to compare treatment groups.

Subcutaneous Xenograft Protocol

Tumor cells grown *in vitro* were harvested with Trypsin-EDTA (Invitrogen), washed $1 \times$ with PBS, and resuspended in Matrigel (BD Biosciences, Bedford, MA) to a final concentration of 10^7 per mL. Six- to 8-week-old female athymic mice were injected s.c. in the suprascapular region with 0.5 mL of the cell suspension. Animals were dosed twice weekly with antibodies diluted in PBS via i.p. or i.v. injection beginning on the day of implant or following a period of tumor establishment. Tumor volume was measured twice weekly using the formula: length \times width \times height \times 0.5. The percent reduction in tumor growth was calculated using the formula: [(control group average volume – treatment group average volume) / control group average volume] \times 100, at each time point reported. Statistical analysis by ANOVA and Student's two-tailed t test were used to compare treatment groups.

Results

RAAG12 Is a N-Linked Carbohydrate Epitope

Western blot analysis showed the RAAG12 epitope was present on multiple membrane-associated proteins over a molecular weight range from ~ 25 to >250 kDa (data not shown). Digestion of RAAG12-bearing proteins purified from COLO 205 cells with a range of enzymes showed KID3 reactivity decreased following treatment with *N*-glycanase (PNGaseF; Fig. 1A). Treatment with *N*-glycanase and fucosidase ($\alpha 1$ -3,4 fucosidase or $\alpha 1$ -2,4,6 fucosidase) further decreased KID3 reactivity. Treatment with endo-*O*-glycanase or sialidase (sialidase A/NANase III) did not alter KID3 reactivity. Additionally, treatment with Pronase did not alter KID3 reactivity (data not shown). These studies suggested that RAV12 bound exclusively to an N-linked carbohydrate moiety and prompted examination of whether RAV12 recognized known tumor-associated carbohydrate antigens.

A survey of tumor-associated glycans showed that antibodies to sialidase-sensitive carbohydrate antigens CA 19-9, CA 50, CA 242, and anti-Le^a antibody PR4D2 were reactive with RAAG12 isolated from COLO 205 cells, showing that the Le^a antigen, or a closely related glycan, is present on RAAG12-bearing proteins (Fig. 1B). Antibodies against Le^b, Le^x, and Le^y were nonreactive. These observations led to the examination of KID3 reactivity with a series of Le^a-related glyco-analogues. Analysis of glyco-analogues showed that KID3 and PR4D2 were reactive to the Le^a-related analogue LNFPII (Fig. 1C). As

shown in Fig. 1D, KID3 binding to LNFPII was strongly inhibited by lacto-*N*-tetraose, Gal β -3GlcNAc, and lacto-*N*-hexaose (all three lack the fucose moiety) but was not inhibited by Le^a or lacto-*N*-neotetraose. Lactose alone was not supportive of RAV12 binding. Taken together, these data suggest that the RAV12-binding site on RAAG12 consists minimally of Gal β 1-3GlcNAc β 1-3Gal.

RAAG12 Is Highly Expressed by Gastrointestinal Adenocarcinoma Tumors

RAAG12 is expressed predominantly by adenocarcinomas. Colorectal, gastric, and pancreatic adenocarcinomas express RAAG12 most frequently and with the most uniform expression. Photomicrographs of representative primary human tumors are shown in Fig. 2A. As shown in Table 1A, more than 90% of tumors of colorectal, gastric, and pancreatic origin expressed RAAG12, and a majority of these tumors (64–75%) exhibited uniform RAAG12 expression (staining of $>75\%$ of tumor cells present). A number of other adenocarcinomas, including breast, prostate, lung, kidney, and ovarian, showed overall frequencies of RAAG12 expression between 30% and 65%.

The high proportion of RAAG12-positive adenocarcinomas prompted further immunohistochemical studies. A strong correlation was observed between RAAG12 expression in primary and metastatic colorectal carcinomas (Table 1B). Analysis of colorectal cancer samples from 94 primary and 24 metastatic tumors (11 from lymph nodes and 13 from distant sites) showed that 91% of primary lesions and 83% of metastatic lesions were positive for RAAG12 expression, with 66% and 54%, respectively, expressing RAAG12 with high intensity. More than 80% of 11 matched primary and metastatic lesions showed equivalent pattern and intensity of staining (data not shown).

Immunohistochemical analysis showed limited RAAG12 expression on normal human tissues. No expression of RAAG12 was seen on connective tissue or tissues from the cardiovascular, endocrine, hematolymphatic, neuromuscular, and central nervous systems. RAAG12 expression was observed in exocrine epithelia in multiple tissues, which in general are the tissues from which the corresponding RAAG12-positive adenocarcinomas arise. The most frequent and intense RAAG12 expression was seen in mucosal epithelium of the gastrointestinal tract, biliary epithelium, mucosal stratified squamous epithelium, pancreatic acinar/ductal epithelium, skin sweat glands/ducts, and glandular/ductal breast epithelium. The majority of RAAG12 in cells from these normal epithelial tissues was localized to the cytoplasm. Membrane expression in gastrointestinal and ductal epithelium was predominantly restricted to the apical surface in normal tissue samples, whereas RAAG12 expression in adenocarcinomas tended to be throughout the membrane and accessible on the surface (Fig. 2B).

RAV12 Is Directly Cytotoxic to COLO 205 Cells *In vitro* via Oncosis

Initial studies showed that the murine KID3 antibody was cytotoxic to the RAAG12-expressing COLO 205 cell line, and that the bioactivity was retained by the RAV12

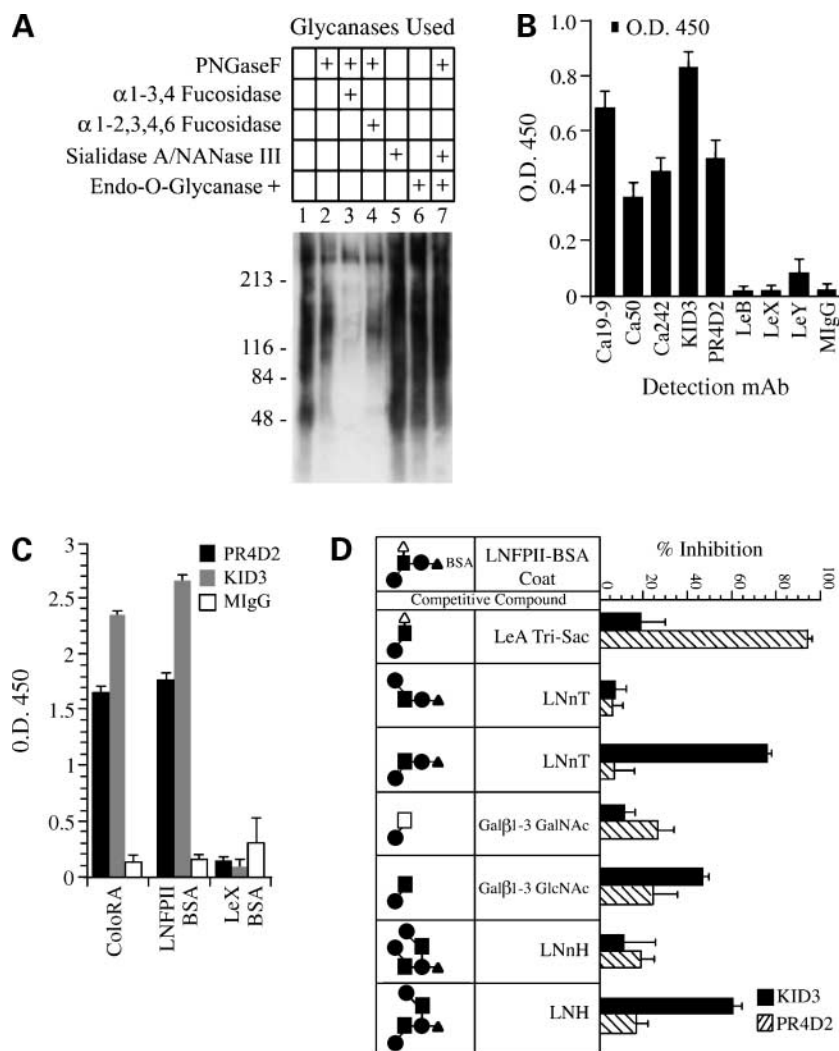


Figure 1. RAAG12 is an N-linked carbohydrate epitope present on multiple proteins. **A**, Western blot of SDS-PAGE resolved RAAG12-bearing proteins purified from COLO 205 cells (ColoRA). Purified protein samples were treated with glycanases in the combinations illustrated in the associated table. Representative of four independent experiments. **B**, ELISA assay to detect binding of the indicated antibodies to ColoRA immobilized on 96-well plates. Mouse IgG (MIgG) was used as a negative control. Representative of two independent experiments done in triplicate wells. **C**, ELISA bridging study to detect binding of KID3 or PR4D2 antibody to ColoRA or LNFPII-BSA immobilized on 96-well plates. Mouse IgG was used as a negative control. Representative of six independent experiments done in quadruplicate wells. **D**, ELISA assay to detect competitive inhibition by a panel of glyco-analogues for binding of KID3 or PR4D2 antibody to the glyco-analogue LNFPII-BSA immobilized on 96-well plates. Adjacent table is a representation of the compounds: ●, Gal; ■, GlcNAc; ▲, Glc; □, GalNAc; △, Fuc. Representative of four independent experiments. LNT, lacto-*N*-tetraose; LNNT, lacto-*N*-neotetraose; LNT, lacto-*N*-tetraose; LNNT, lacto-*N*-neohexaose; LNNT, lacto-*N*-hexaose.

chimeric antibody. As shown in Fig. 3A, RAV12 induced a concentration-dependent cytotoxicity on COLO 205 cells with an ED₅₀ of 7 μ g/mL. RAV12-mediated cytotoxicity seems to require cross-linking of cellular components: Fab fragments of RAV12 did not induce cytotoxicity, whereas cross-linking of the Fab fragments with a secondary antibody restored the cytotoxic activity to the level of the intact antibody (data not shown). Following RAV12 treatment, COLO 205 cells *in vitro* seemed to undergo a type of regulated cell death termed oncosis. The hallmarks of oncosis are cell and organelle swelling, vacuolization, and increased membrane permeability, followed by cell lysis (4, 9, 10). Microscopic examination revealed that COLO 205 cells underwent rapid swelling within 1 h following RAV12 treatment (Fig. 3B). Double staining for RAV12 and filamentous-actin showed that RAV12 was associated with the plasma membrane, and that treatment with RAV12 caused disruption of the actin cytoskeleton. Time-lapse microscopy using KID3 revealed that cellular swelling led to membrane leakage and/or rupture follow-

ing treatment (Fig. 3C). Elevated lactate dehydrogenase was detected in the medium within 30 min of antibody addition, indicative of membrane rupture (data not shown).

Although the molecular mechanisms underlying oncosis have not been fully elucidated, oncosis may result from dysregulated membrane ion channels and decreased levels of intracellular ATP, which leads to sodium influx, cell swelling, and lysis (11). Consistent with these observations, KID3-induced cytotoxicity was attenuated by reducing the extracellular sodium concentration. COLO 205 cells exposed to a low sodium-containing medium (15 mmol/L sodium) for 24 h were resistant to KID3-induced lysis, whereas cells cultured in physiologic sodium-containing medium remained sensitive to KID3 (Fig. 3D). Markers of apoptotic cell death, including Annexin V staining and terminal deoxynucleotidyl transferase biotin-dUTP nick end labeling or changes in cell cycle, were not observed following KID3 treatment (data not shown).

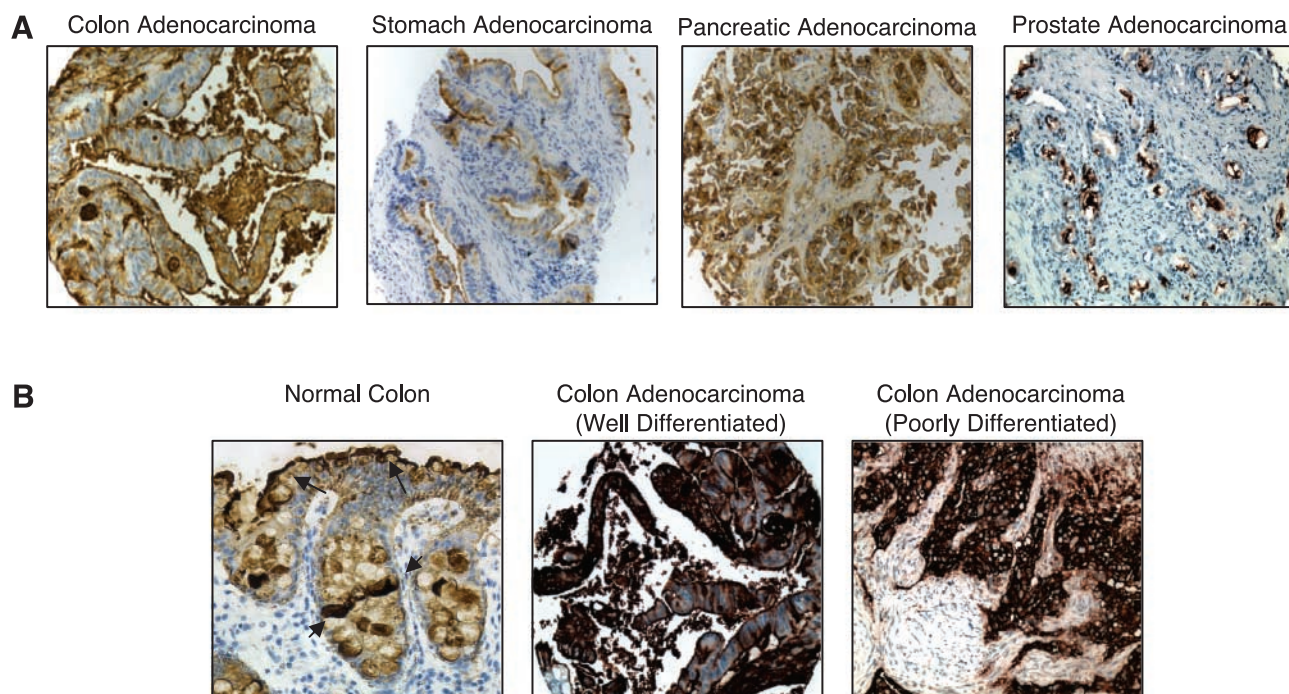


Figure 2. RAAG12 expression pattern in normal colon and adenocarcinoma tumors. FFPE specimens were stained with RAV12 (5 $\mu\text{g}/\text{mL}$) and counterstained with hematoxylin. **A**, examples of gastrointestinal adenocarcinoma types with high RAAG12 expression and an example of a prostate adenocarcinoma with moderate RAAG12 expression. **B**, example of a normal colon with primarily cytoplasmic RAAG12 expression (arrowheads of goblet cells) and on the apical membrane of the surface colonic epithelium (arrows), a well-differentiated colon adenocarcinoma with increased basolateral RAAG12 expression, and a poorly differentiated colon adenocarcinoma exhibiting entire membrane RAAG12 expression. All images captured at $\times 200$ magnification.

RAV12 Inhibits Tumor Growth in Multiple Gastrointestinal Xenograft Models

Studies with KID3 in the subrenal capsule model established that tumors derived from tumor cell lines with high uniform expression of RAAG12 (COLO 201, COLO 205, SNU-16, and SU.86.86) were sensitive to treatment with KID3, whereas cell lines expressing low levels of RAAG12 (<10% of cells staining; A549, HT-29, and CaKi-2) were insensitive. Based on these results, a series of subrenal capsule xenograft studies were conducted to assess the *in vivo* bioactivity of RAV12. A bridging study comparing KID3 and RAV12 showed comparable activity toward COLO 201 xenografts in the subrenal capsule model (data not shown). Dose response studies with RAV12 showed that treatment decreased tumor size by 60% relative to control at 1 mg/kg, the lowest dose examined, whereas doses of 25 mg/kg decreased tumor size by more than 92%, and doses of 50 mg/kg eliminated detectable COLO 201 tumors in the majority of treated animals (Fig. 4A). RAV12 treatment caused a similar dose-dependent reduction of tumor size in subrenal capsule xenografts derived from SU.86.86 tumor cells (Fig. 4B).

Because RAAG12 expression was observed in the mucosal epithelium of a limited subset of normal tissues, we used the subrenal capsule model to assess whether antibody treatment was cytotoxic toward normal colon tissue. Normal fetal colon epithelium was matured under

the mouse kidney capsule until it achieved a cellular architecture and RAAG12 antigen expression pattern similar to the adult human colon (12). The mature normal human colon tissue was not affected by KID3 treatment, whereas COLO 205 tumor xenografts implanted under the contralateral kidney capsule (as done in the experiments shown in Fig. 4) were reduced or eliminated following KID3 treatment.¹

Antitumor activity was also observed with RAV12 in s.c. xenograft models. As shown in Fig. 5A, administration of 50 mg/kg RAV12 i.p. twice weekly beginning on the day of SNU-16 gastric tumor implantation suppressed tumor growth by 69% relative to control at day 25 after implantation. Similarly, animals given 50 mg/kg RAV12 i.p. twice weekly beginning on the day of COLO 205 implantation showed a 74% decrease in tumor growth at the end of study (Fig. 5B). In contrast, A549 tumors, which express low, heterogeneous levels of RAAG12, were not affected by RAV12 treatment at 50 mg/kg (Fig. 5C). The dose response of RAV12 was evaluated using SNU-16 s.c. xenografts. RAV12 was administered at 3, 10, 30, and 100 mg/kg i.v. on the day of tumor implantation. As shown in Fig. 5D, administration of 3 mg/kg RAV12 resulted in a 71% reduction in tumor growth of SNU-16 xenografts on

¹ P. Young and J.P. Mather, in preparation.

day 22. The 10 mg/kg dose level resulted in an 80% reduction in tumor growth on day 22, which was not significantly improved by higher dose levels nor was it significantly different from the 3 mg/kg dose. The i.v. dosing study with SNU-16 xenografts was repeated with doses of 1, 3, and 10 mg/kg of RAV12. The 3 mg/kg dose of RAV12 caused a 82% reduction in tumor growth, which was not statistically different from the 10 mg/kg dose group (data not shown). Based on these results, RAV12 antitumor activity was examined with SNU-16 s.c. xenografts in an established tumor mode. Twice weekly i.p. treatment of established SNU-16 xenografts (150–200 mm³ tumor volume) with RAV12 at 10 mg/kg completely suppressed tumor growth over the initial 15 days of treatment and resulted in an overall decrease in tumor growth of 66% at the end of the study (Fig. 5E). Treatment of the established SNU-16 xenografts with RAV12 at 50 mg/kg i.p. led to a similar pattern of reduced tumor volume with an overall reduction of 58% at the end of the study.

Discussion

Many therapeutic antibodies have been developed for the treatment of cancer. However, only a small subset of these antibodies has been shown to elicit direct cytotoxic activity. The data presented here show that RAV12 is able to exert a direct cytotoxic effect *in vitro* against human colorectal adenocarcinoma cells. COLO 205 cells exposed to RAV12 *in vitro* undergo rapid membrane swelling and lysis, hallmarks of oncosis. RAV12-induced cytotoxicity *in vitro* occurs in both serum-containing and serum-free cell culture, supporting the conclusion that RAV12 had direct

cytotoxic activity on tumor cells (data not shown). The cytotoxic activity observed for RAV12 *in vitro* was reflected in the potent antitumor activity observed in multiple gastrointestinal xenografts *in vivo*, including colon, gastric, and pancreatic tumors. Significant antitumor activity was observed with RAV12 at the 1 mg/kg dose in the subrenal capsule model, where treatment started 2 days following tumor implantation, and increased to a 92% reduction in tumor size at the 25 mg/kg dose. Treatment with 50 mg/kg or greater of RAV12 reduced tumors to undetectable levels in many animals. Consistent with the activity observed in the subrenal capsule studies, potent antitumor activity was also observed in both preventative and established s.c. xenograft studies. For SNU-16 tumors, the 3 mg/kg dose of RAV12 initiated on the day of tumor implantation resulted in a 71% decrease in tumor growth at the end of study, whereas a 10 mg/kg dose of RAV12 initiated after tumors had established to 150 to 200 mm³ led to a 68% decrease in tumor growth at the end of study. We are expanding our xenograft studies to investigate the potential for additive or synergistic effects of approved standard of care therapies.

The term oncosis was initially proposed to describe ischemic death of osteocytes with swelling (9). Oncosis has been recently adapted by Majno et al. to describe a mechanism of cell death distinct from the more extensively studied cell death mechanism of apoptosis (10). Although apoptosis is characterized by cell shrinkage, chromatin condensation, and formation of apoptotic bodies, oncosis is characterized by rapid cell swelling, organelle swelling, membrane permeability, and cell lysis. Cell death by apoptosis leads to necrosis with karyorrhexis, whereas cell death by oncosis may result in necrosis with karyolysis

Table 1.

A. Major human tumor types with high frequencies of uniform RAAG12 expression

Tumor type	Proportion positive (%)	No. (%) samples expressing RAAG12*			
		≥75%	50-74%	11-49%	<10%
Colorectal carcinoma	107/119 (90)	76 (64)	9 (7)	9 (7)	13 (11)
Stomach adenocarcinoma	88/94 (94)	63 (67)	3 (3)	13 (14)	9 (10)
Pancreas adenocarcinoma	16/16 (100)	12 (75)	3 (19)	1 (6)	0

B. Frequency of RAAG12 expression on primary and metastatic human colorectal tumors

Colorectal tumors	Proportion positive (%)	No. (%) samples expressing RAAG12 [†]			
		≥75%	50-74%	11-49%	<10%
Primary lesions	86/94 (91)	62 (66)	7 (7)	7 (7)	10 (11)
Metastases	20/24 (83)	13 (54)	2 (8)	2 (8)	3 (13)
Recurrent tumors	1/1 (100)	1/1 (100)	0	0	0

*Percentages in parentheses were calculated as number of RAAG12-positive samples for each quartile divided by total number of samples for the specific tumor type (percent negative samples not shown).

[†] Percentages in parentheses were calculated as number of RAAG12-positive samples for each quartile divided by the total number of samples in each tumor type (percent negative samples not shown).

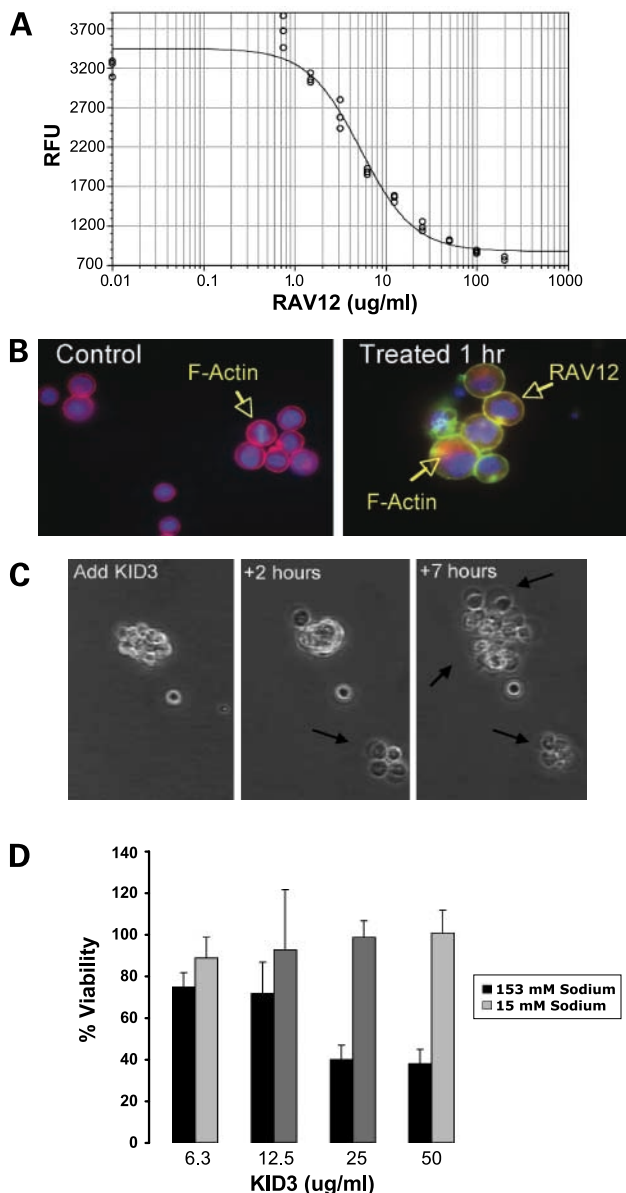


Figure 3. RAV12 is directly cytotoxic to COLO 205 colon tumor cells *in vitro*. **A**, exposure to RAV12 induces dose-dependent cytotoxicity of COLO 205 cells. Cells were incubated with RAV12 for 4 d at the indicated concentrations before addition of the Alamar Blue reagent. Viable cell number of triplicate samples is expressed as relative fluorescent units (RFU). **B**, RAV12 treatment rapidly induces cell swelling and disrupts actin cytoskeleton. Localization of filamentous actin (*F-actin*; control and RAV12 treated cultures) or RAV12 (RAV12-treated culture only). Images from both cultures captured at $\times 40$ magnification. **C**, KID3 induces rapid cellular swelling and membrane rupture. Time-lapse video microscopy images of KID3-treated COLO 205 cells. Cultures at 0, 2, and 7 h following KID3 addition. Clusters of COLO 205 cells can be seen undergoing membrane swelling and cell lysis (arrows). **D**, reduced extracellular sodium protects COLO 205 cells from KID3-induced cytotoxicity. KID3-treated COLO 205 cells were cultured in the presence of normal sodium (153 mmol/L) or low sodium (15 mmol/L) containing medium. Twenty-four hours following treatment, the number of cells present with intact membranes was determined by visual assessment and expressed as % viability relative to untreated cultures. Representative of two independent experiments.

(9, 10). Thus, postmortem examination of both apoptotic and oncotic cells may reveal cellular and/or molecular characteristics of necrosis. An emerging view is that cell death in many systems previously described as necrosis may result from activation of nonapoptotic cell death mechanisms such as oncosis. Two examples of antibodies that mediate cell death resembling oncosis have been reported. The RE2 antibody is cytotoxic to lymphocytes by a mechanism distinct from apoptosis (13). Although the molecular target of the RE2 antibody remains unknown, RE2-mediated cell death was accompanied by rapid formation of plasma membrane pores. Similar to our observations with RAV12, RE2-mediated cell death occurred in the absence of complement and required cross-linking of cell surface components. A second antibody directed against porimin, a 110-kDa cell surface receptor, induces complement-independent cell death with features of oncosis. Anti-porimin-mediated cell death was preceded by rapid cell aggregation and pore formation on the plasma membrane, cell swelling, and membrane blebbing (14, 15). Defining the molecular entities mediating oncosis in these systems may aid in understanding the relationship between these oncotic cell death signals and whether they share common molecular pathways.

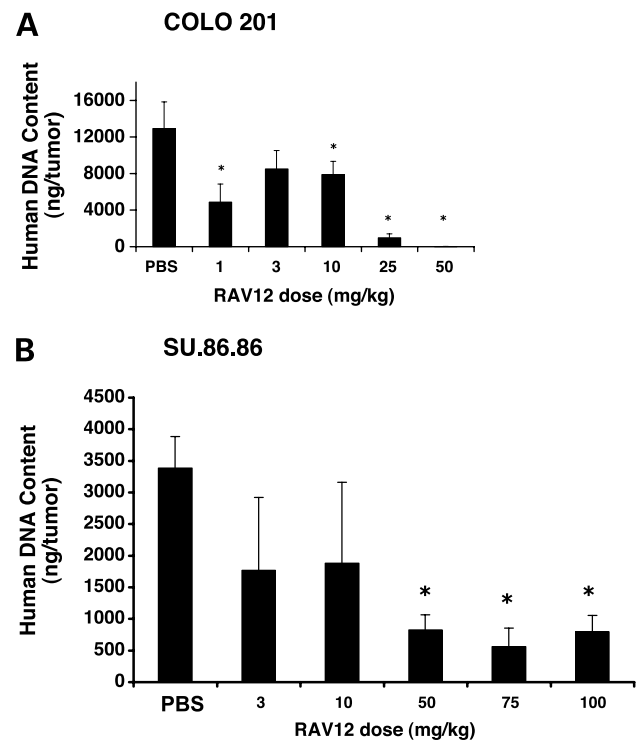


Figure 4. RAV12 inhibits tumor growth of subrenal capsule gastrointestinal tumor xenografts: 5×10^5 (A) COLO 201 colon or (B) SU.86.86 pancreatic tumor cells were suspended in collagen and surgically implanted beneath the renal capsule of athymic mice. Beginning on day 2 after implantation, mice were dosed i.p. with RAV12 or an equivalent volume of PBS thrice weekly. On day 16, animals were sacrificed, and tumors were collected and analyzed by quantitative PCR for human DNA to quantify tumor mass. Columns, mean for four to five mice per group; bars, SD. *, $P < 0.05$ (two-tailed Student's *t* test).

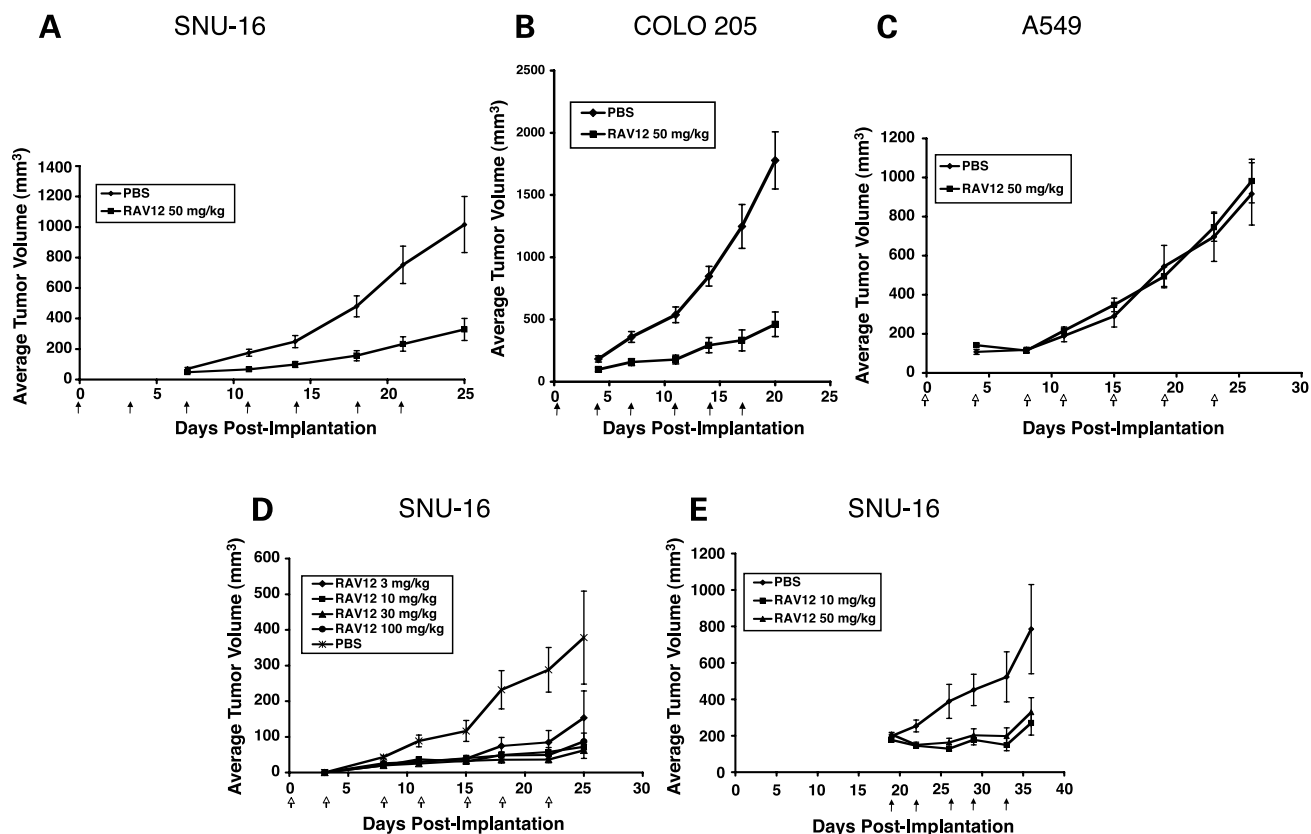


Figure 5. RAV12 inhibits tumor growth of s.c. gastrointestinal tumor xenografts in both a preventative and established tumor mode. Athymic mice were implanted s.c. with 5×10^6 of the indicated tumor cells in Matrigel and treated with RAV12 twice weekly (arrows) at the indicated doses. **A to D**, treatment with RAV12 beginning on the day of tumor implantation. **E**, treatment with RAV12 initiated when the average tumor volume reached 150 to 200 mm³. Tumors were measured twice weekly. **A to C** and **E**, animals were dosed i.p. **D**, animals were dosed i.v. Points, mean for 15 animals per group; bars, SE. **A**, $P < 0.01$, day 25; **B**, $P < 0.01$, day 21; **D**, $P < 0.008$ for all four treatment groups, day 22; **E**, $P < 0.05$ for both treatments, day 33. All P s determined using two-tailed Student's t test.

Oncosis occurs in numerous human diseases, including acute renal and liver failure, myocardial infarction, and stroke (16). In some cases, cell death is accompanied by inflammation due to the release of intracellular contents of oncotic cells. Although the molecular mechanisms of oncosis are not fully understood, the nature and sequence of events in cells undergoing oncosis is beginning to emerge. In the case of hepatocytes exposed to menadione or KCN, Carini et al. (17) observed that the intracellular concentrations of sodium and ATP can play a key role in determining cellular fate. Treatment of hepatocytes with menadione or KCN caused a drop in intracellular ATP. In the presence of sodium in the bathing medium, most cells died following treatment; however, when sodium was removed from the bathing medium, the cells did not swell or lose viability. In this system, the combination of low intracellular ATP and high intracellular sodium were necessary for oncosis. Consistent with this observed role of sodium influx in oncosis, we found that RAV12-mediated lysis could be attenuated by reducing the extracellular sodium concentration.

Immunohistochemical analysis showed that adenocarcinomas, especially colorectal, gastric, and pancreatic adenocarcinomas, have a high prevalence of strong, uniform RAAG12 expression. Additional studies have shown that both primary and metastatic lesions in colon cancer have similar frequencies of strong, uniform RAAG12 expression, suggesting that the RAAG12 glycoepitope persists in metastatic disease. In gastrointestinal adenocarcinomas, RAAG12 membrane localization progresses from apical and increased basolateral expression in well to moderately differentiated tumors to expression across the entire membrane surface in poorly differentiated and diffuse tumors. Conversely, RAAG12 expression on normal polarized epithelia is predominantly localized to the cytoplasm or apical membrane surfaces. We hypothesize that the differential localization of RAAG12 in tumor versus normal epithelium may translate to preferential access of tumors to i.v. administered RAV12.

Aberrant glycosylation has been observed in human cancers and is thought to play a role in oncogenic transformation, tumor invasion, and metastasis (18–20). Many of the carbohydrate epitopes resulting from aberrant

glycosylation have the potential to be tumor-associated antigens that are either tumor specific or overexpressed on tumors and may serve as promising targets for cancer therapy. The Lewis blood group family of carbohydrate antigens represents a prototypical tumor-associated antigen. Expression of Lewis blood group antigens on normal adult tissues is restricted to granulocytes and differentiated epithelial cells but is overexpressed on carcinomas. In the case of Le^y, abundant expression has been reported on carcinomas of the colon, breast, ovary, lung, pancreas, and prostate (21), and this expression has been correlated with increased invasion and metastasis and decreased survival rates in patients (22, 23). Our studies using glyco-analogues showed that KID3 is reactive to the Le^a-related analogue LNFPII. Competition studies showed that the Le^a triose was insufficient to support KID3 binding, whereas lacto-N-tetraose completely inhibited KID3/LNFPII interaction. Lactose (Galβ1-4Glc) alone was also not supportive of KID3 binding as all glyco-analogues tested were lactose-based derivatives. Taken together, our results support the conclusion that the RAAG12 glycotope is a N-linked type 1 glycan chain consisting minimally of Galβ1-3GlcNAcβ1-3Gal and represents a potentially novel tumor-associated carbohydrate antigen.

The protein molecular entities that confer cellular sensitivity to RAV12 remain unidentified. We hypothesize that cell sensitivity to RAV12 may be mediated by a subset of RAAG12-bearing proteins. The requirement for cross-linking of RAV12 Fab fragments for cytotoxicity is consistent with the hypothesis that RAV12 cross-links RAAG12 epitopes, leading to antibody-receptor complex internalization and initiation of pro-oncotic signals. A recent report by Klinger et al. (24) reported that ErbB1 and ErbB2 are modified with Le^y on human breast and epidermoid tumor cells, and monoclonal anti-Le^y antibodies block epidermal growth factor- and heregulin-stimulated phosphorylation of mitogen-activated protein kinase in these cells. The inhibition of ErbB-induced downstream signaling was noncompetitive, and anti-Le^y antibody-mediated rerouting of receptor trafficking has been proposed as a mechanism for the inhibitory activity. We are initiating studies to survey RAAG12-bearing cell surface proteins on responsive and nonresponsive cell lines in an attempt to identify differentially expressed molecular targets that contribute to RAV12 sensitivity.

In conclusion, we have generated a chimeric monoclonal antibody (RAV12) that induces oncotic cell death *in vitro* and exhibits potent antitumor activity *in vivo* against multiple human tumor cell lines of gastrointestinal origin. Based on the biological properties of RAV12, the expression pattern of the RAAG12 glycotope antigen, and the safety profile observed in a repeat-dose primate toxicology study, a phase I/IIA clinical trial was designed to examine safety, pharmacokinetics, and preliminary efficacy in patients with relapsed, refractory adenocarcinoma of gastrointestinal (gastroesophageal, pancreatic, and colorectal) origin or other origin if proven to express RAAG12 by immunohistochemistry. This trial is currently accruing patients.

Acknowledgments

We thank Drs. Gordon Vehar and Stanford Steward for helpful discussions and critical review of the article, the Raven Biotechnologies scientific staff for expert technical assistance, and Linda Davis for assistance with preparation of the article.

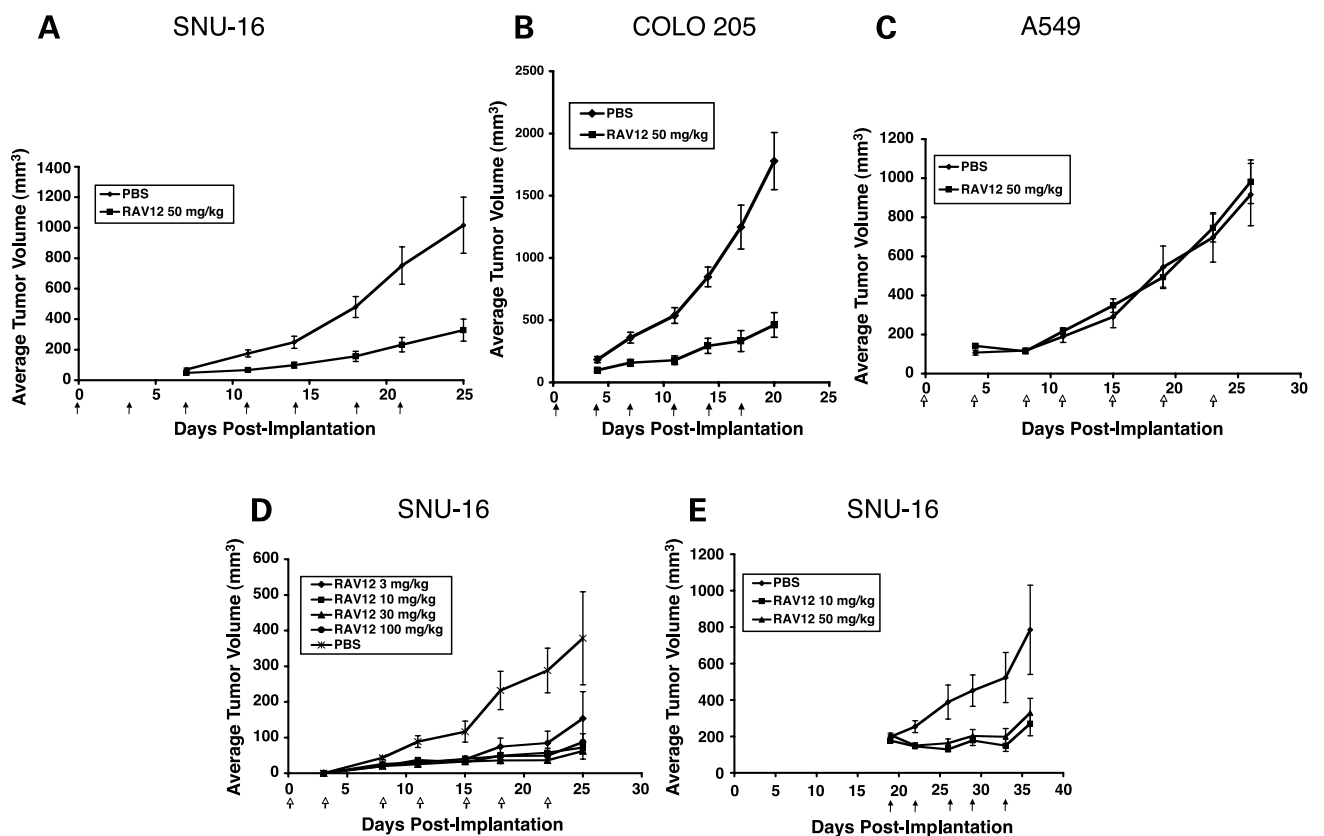
References

- Stephan JP, Roberts PE, Bald L, et al. Selective cloning of cell surface proteins involved in organ development: epithelial glycoprotein is involved in normal epithelial differentiation. *Endocrinology* 1999;140:5841–54.
- Li R, Gao W-Q, Mather JP. Multiple factors control the proliferation and differentiation of rat early embryonic (day 9) neuroepithelial cells. *Endocrine* 1996;5:205–17.
- Li R, Phillips DM, Moore A, Mather JP. Follicle-stimulating hormone induces terminal differentiation in a predifferentiated rat granulosa cell line (ROG). *Endocrinology* 1997;138:2648–57.
- Zong WX, Thompson CB. Necrotic death as a cell fate. *Genes Dev* 2006;20:1–15.
- Harlow E, Lane D. *Antibodies: a laboratory manual*. New York: Cold Spring Harbor Laboratory Press; 1988.
- Sambrook J, Fritsch E, Maniatis T. *Molecular cloning, a laboratory manual*. New York: Cold Spring Harbor Laboratory Press; 1989.
- Parmar H, Young P, Emerman JT, Neve RM, Dairkee S, Cunha GR. A novel method for growing human breast epithelium *in vivo* using mouse and human mammary fibroblasts. *Endocrinology* 2002;143:4886–96.
- Davies B, Fried M. The L19 ribosomal protein gene (RPL19): gene organization, chromosomal mapping, and novel promoter region. *Genomics* 1995;25:372–80.
- Trump BF, Berezsky IK, Chang SH, Phelps PC. The pathways of cell death: oncosis, apoptosis, and necrosis. *Toxicol Pathol* 1997;25:82–8.
- Majno G, Joris I. Apoptosis, oncosis, and necrosis. An overview of cell death. *Am J Pathol* 1995;146:3–15.
- Barros LF, Hermsilla T, Castro J. Necrotic volume increase and the early physiology of necrosis. *Comp Biochem Physiol A Mol Integr Physiol* 2001;130:401–9.
- Mather JP, Young PF, inventors; Raven Biotechnologies, Inc., assignee. Animal model for toxicology and dose prediction. United States patent US 20,040,045,045. 2004 March 4.
- Matsuoka S, Asano Y, Sano K, et al. A novel type of cell death of lymphocytes induced by a monoclonal antibody without participation of complement. *J Exp Med* 1995;181:2007–15.
- Zhang C, Xu Y, Gu J, Schlossman SF. A cell surface receptor defined by a mAb mediates a unique type of cell death similar to oncosis. *Proc Natl Acad Sci U S A* 1998;95:6290–5.
- Ma F, Zhang C, Prasad KV, Freeman GJ, Schlossman SF. Molecular cloning of Porimin, a novel cell surface receptor mediating oncotic cell death. *Proc Natl Acad Sci U S A* 2001;98:9778–83.
- Liu X, Van Vleet T, Schnellmann RG. The role of calpain in oncotic cell death. *Annu Rev Pharmacol Toxicol* 2004;44:349–70.
- Carini R, Autelli R, Bellomo G, Albano E. Alterations of cell volume regulation in the development of hepatocyte necrosis. *Exp Cell Res* 1999;248:280–93.
- Hakomori S. Glycosylation defining cancer malignancy: new wine in an old bottle. *Proc Natl Acad Sci U S A* 2002;99:10231–3.
- Fuster MM, Esko JD. The sweet and sour of cancer: glycans as novel therapeutic targets. *Nat Rev Cancer* 2005;5:526–42.
- Dube DH, Bertozzi CR. Glycans in cancer and inflammation: potential for therapeutics and diagnostics. *Nat Rev Drug Discov* 2005;4:477–88.
- Hellstrom I, Garrigues HJ, Garrigues U, Hellstrom KE. Highly tumor-reactive, internalizing, mouse monoclonal antibodies to Le(y)-related cell surface antigens. *Cancer Res* 1990;50:2183–90.
- Hakomori S. Tumor malignancy defined by aberrant glycosylation and sphingo(glyco)lipid metabolism. *Cancer Res* 1996;56:5309–18.
- Muramatsu T. Carbohydrate signals in metastasis and prognosis of human carcinomas. *Glycobiology* 1993;3:291–6.
- Klinger M, Farhan H, Just H, et al. Antibodies directed against Lewis-Y antigen inhibit signaling of Lewis-Y modified ErbB receptors. *Cancer Res* 2004;64:1087–93.

Correction

Article on RAV12 antibody, oncosis, and antitumor activity

In the article on RAV12 antibody, oncosis, and antitumor activity in the March 2007 (1) issue, some of the data in part E of Fig. 5 appeared incorrectly. The corrected Fig. 5 appears below.



Reference

1. Loo D, Pryer N, Young P, Liang T, Coberly S, King KL, Kang K, Roberts P, Tsao M, Xu X, Potts B, Mather JP. The glycotope-specific RAV12 monoclonal antibody induces oncosis *in vitro* and has antitumor activity against gastrointestinal adenocarcinoma tumor xenografts *in vivo*. *Mol Cancer Ther* 2007;6:856 - 65.

Molecular Cancer Therapeutics

The glycotope-specific RAV12 monoclonal antibody induces oncosis *in vitro* and has antitumor activity against gastrointestinal adenocarcinoma tumor xenografts *in vivo*

Deryk Loo, Nancy Pryer, Peter Young, et al.

Mol Cancer Ther 2007;6:856-865.

Updated version Access the most recent version of this article at:
<http://mct.aacrjournals.org/content/6/3/856>

Cited articles This article cites 21 articles, 8 of which you can access for free at:
<http://mct.aacrjournals.org/content/6/3/856.full#ref-list-1>

Citing articles This article has been cited by 10 HighWire-hosted articles. Access the articles at:
<http://mct.aacrjournals.org/content/6/3/856.full#related-urls>

E-mail alerts [Sign up to receive free email-alerts](#) related to this article or journal.

Reprints and Subscriptions To order reprints of this article or to subscribe to the journal, contact the AACR Publications Department at pubs@aacr.org.

Permissions To request permission to re-use all or part of this article, use this link
<http://mct.aacrjournals.org/content/6/3/856>.
Click on "Request Permissions" which will take you to the Copyright Clearance Center's (CCC) Rightslink site.